



**HAL**  
open science

## Influence on cell death of high frequency motion of magnetic nanoparticles during magnetic hyperthermia experiments

Nicolas Hallali, Pascal Clerc, Daniel Fourmy, Véronique Gigoux, Julian Carrey

► **To cite this version:**

Nicolas Hallali, Pascal Clerc, Daniel Fourmy, Véronique Gigoux, Julian Carrey. Influence on cell death of high frequency motion of magnetic nanoparticles during magnetic hyperthermia experiments. Applied Physics Letters, 2016, 109 (3), pp.032402. hal-01983252

**HAL Id: hal-01983252**

**<https://hal.insa-toulouse.fr/hal-01983252>**

Submitted on 16 Jan 2019

**HAL** is a multi-disciplinary open access archive for the deposit and dissemination of scientific research documents, whether they are published or not. The documents may come from teaching and research institutions in France or abroad, or from public or private research centers.

L'archive ouverte pluridisciplinaire **HAL**, est destinée au dépôt et à la diffusion de documents scientifiques de niveau recherche, publiés ou non, émanant des établissements d'enseignement et de recherche français ou étrangers, des laboratoires publics ou privés.

# Influence on cell death of high frequency motion of magnetic nanoparticles during magnetic hyperthermia experiments

Cite as: Appl. Phys. Lett. **109**, 032402 (2016); <https://doi.org/10.1063/1.4958989>

Submitted: 07 June 2016 . Accepted: 06 July 2016 . Published Online: 18 July 2016

N. Hallali , P. Clerc, D. Fourmy, V. Gigoux , and J. Carrey



View Online



Export Citation



CrossMark

## ARTICLES YOU MAY BE INTERESTED IN

[Fundamentals and advances in magnetic hyperthermia](#)

Applied Physics Reviews **2**, 041302 (2015); <https://doi.org/10.1063/1.4935688>

[Magnetic nanoparticles for enhancing the effectiveness of ultrasonic hyperthermia](#)

Applied Physics Letters **108**, 263701 (2016); <https://doi.org/10.1063/1.4955130>

[Simple models for dynamic hysteresis loop calculations of magnetic single-domain nanoparticles: Application to magnetic hyperthermia optimization](#)

Journal of Applied Physics **109**, 083921 (2011); <https://doi.org/10.1063/1.3551582>



**Measure Ready**  
**M91 FastHall™ Controller**

A revolutionary new instrument  
for complete Hall analysis

 Lake Shore  
CRYOTRONICS



## Influence on cell death of high frequency motion of magnetic nanoparticles during magnetic hyperthermia experiments

N. Hallali,<sup>1,2</sup> P. Clerc,<sup>2,3</sup> D. Fourmy,<sup>2,3</sup> V. Gigoux,<sup>2,3</sup> and J. Carrey<sup>2,a)</sup>

<sup>1</sup>CEA Tech MiPy, INSA, Bâtiment 8, 135 avenue de Rangueil, F-31432 Toulouse, France

<sup>2</sup>Université de Toulouse; INSA; UPS; LPCNO (Laboratoire de Physique et Chimie des Nano-Objets),

135 avenue de Rangueil, F-31077 Toulouse, France and CNRS; UMR 5215; LPCNO, F-31077 Toulouse, France

<sup>3</sup>INSERM ERL1226, RTTC (Receptology and Targeted Therapy of Cancers), 1 avenue Jean Poulhès, F-31432 Toulouse, France

(Received 7 June 2016; accepted 6 July 2016; published online 18 July 2016)

Studies with transplanted tumors in animals and clinical trials have provided the proof-of-concept of magnetic hyperthermia (MH) therapy of cancers using iron oxide nanoparticles. Interestingly, in several studies, the application of an alternating magnetic field (AMF) to tumor cells having internalized and accumulated magnetic nanoparticles (MNPs) into their lysosomes can induce cell death without detectable temperature increase. To explain these results, among other hypotheses, it was proposed that cell death could be due to the high-frequency translational motion of MNPs under the influence of the AMF gradient generated involuntarily by most inductors. Such mechanical actions of MNPs might cause cellular damages and participate in the induction of cell death under MH conditions. To test this hypothesis, we developed a setup maximizing this effect. It is composed of an anti-Helmholtz coil and two permanent magnets, which produce an AMF gradient and a superimposed static MF. We have measured the MNP heating power and treated tumor cells by a standard AMF and by an AMF gradient, on which was added or not a static magnetic field. We showed that the presence of a static magnetic field prevents MNP heating and cell death in standard MH conditions. The heating power of MNPs in an AMF gradient is weak, position-dependent, and related to the presence of a non-zero AMF. Under an AMF gradient and a static field, no MNP heating and cell death were measured. Consequently, the hypothesis that translational motions could be involved in cell death during MH experiments is ruled out by our experiments. *Published by AIP Publishing.*

[<http://dx.doi.org/10.1063/1.4958989>]

In 1979, Gordon *et al.*<sup>1</sup> proposed a novel approach of hyperthermia to eradicate tumors. The purpose was to inject magnetic nanoparticles (MNPs) inside tumors and to apply a high frequency magnetic field (MF) to achieve magnetic hyperthermia (MH). Because the temperature rise of a tumor depends on its size and of MNP concentration,<sup>2</sup> several theoretical studies showed that MH could reach therapeutic temperature (43 °C) only for tumor with a diameter larger than 3 mm.<sup>3–5</sup> Since, this approach was improved, particularly thanks to therapeutic targeting, which consists in adding chemical ligands on nanoparticle surface to target membrane receptors overexpressed in cancer cells. Following binding to membrane receptors, MNPs are internalized by cells and stored inside vesicles named lysosomes.<sup>6</sup> Finally, an alternating magnetic field (AMF) is applied leading to the death of cancer cells containing MNPs. Surprisingly, it was recently appreciated in several *in-vitro* experiments using low concentration of MNPs in cell culture dishes that there is no need of global increase in the cell temperature to induce tumor cell death.<sup>7–13</sup>

Different hypotheses have been proposed to explain cancer cell death in MH. One of them is based on recent experimental results showing that the temperature rises in the immediate vicinity of the MNPs.<sup>14–17</sup> For instance, in Ref. 17 it was shown that the local temperature increases by

several tens of degree at the MNP surface and decreases drastically at a distance of a few nanometers from the MNP surface. This local heating could damage the lysosomal membrane<sup>13,18</sup> where MNPs are stored and/or catalyze a chemical reaction inside lysosome such as the Fenton reaction.<sup>19,20</sup> Another hypothesis lies in the possibility that the damages caused on cells containing MNPs could be due to a mechanical action generated by the application of the AMF. Two kinds of MNP motions can be induced by AMF application: rotation and translational motion.<sup>5,21,22</sup> This study is focused on the impact on cell viability of the translational motion of MNPs generated within MH experiment. Indeed, as mentioned in Ref. 21, standard AMF inductors used for MH experiments are coils composed of a few turns. Inside these coils, the region with a uniform magnetic field is rather narrow and a high AMF gradient is generated at both sides. Typically, with an AMF of 50 mT at the coil center, an alternating MF gradient (AMFG) of 1 T/m is reached at the coil edge. It was shown that this MF gradient could in principle generate translational magnetic force on MNPs, which would then oscillate mechanically and generate ultrasound waves.<sup>21</sup> Moreover, experimental studies at different frequencies and gradient MF amplitudes showed that ultrasound waves are produced by the MNPs and interact with their biological environment.<sup>23,24</sup> Consequently, in addition to the AMF inducing hyperthermia, MNPs are also exposed to an alternating MF gradient (AMFG) generating MNP translational motion that could cause cellular damages.

<sup>a)</sup>Author to whom correspondence should be addressed. Electronic mail: julian.carrey@insa-toulouse.fr

The aim of this study was to measure the impact on cell viability of translational motion of MNPs when a high-frequency AMFG is applied. A MNP inside an AMFG undergoes a magnetic force  $\vec{F}_M = \mu_0 \nabla H (\vec{\mu} \cdot \vec{e}_z) \vec{e}_z$ , where  $\mu_0 \nabla H$  is the magnetic field gradient amplitude oscillating at the frequency  $f$ ,  $\vec{\mu}$  is the magnetic moment of the nanoparticle, and  $\vec{e}_z$  is the magnetic field gradient direction.<sup>21</sup> To detect the mechanical effect possibly involved in MH, we have conducted cell death experiments where the magnetic force applied to the MNPs was maximized. Experimentally, it consisted in exposing MNPs to a strong AMFG superimposed to a collinear static MF, as suggested in Ref. 21. In addition to maximizing translational movement, a second advantage of using a static MF is that it prevents the heating power of the MNPs. Indeed, the total MF undergone by MNPs is the sum of the static MF and of the AMF. Thus, if the static MF amplitude is higher than the AMF amplitude, the total MF never changes of orientation, so magnetization reversal and heating are both strongly suppressed. Effects of superimposing a static MF to an AMF on MNP magnetization have already been studied theoretically.<sup>25–27</sup> Moreover, several experimental works have shown a heating variation of MNPs as a function of the static MF amplitude.<sup>25,28–30</sup> In summary, the application of a static MF is expected to enhance mechanical effects and to prevent temperature elevation, thus permitting to discriminate between the two mechanisms (local increase of temperature and MNP translational motion) which have been proposed to explain cell death in MH.

For this study, superparamagnetic iron oxide nanoparticles (NIMT FeOdot PEG-Amine, Gecco Dots, Sweden) with a core diameter of 11 nm were used. They were proven to be effective for MH in our previous works.<sup>13,18</sup> To generate the magnetic field in standard MH conditions, a commercial generator and coil (MP12, Fives Celes, France) were used. The coil is made of two turns generating a uniform AMF in its center from 0 to 110 mT at 300 kHz [see Figs. 1(a) and 1(b)]. In order to produce a strong AMFG, this coil was replaced by the custom-made anti-Helmholtz coil presented in Fig. 2(a). This latter coil consists of two contrariwise turns in series producing two identical and opposed AMF at  $f = 393$  kHz. As shown in Fig. 2(b), the two AMF cancel each other out at the coil center generating an AMFG with an amplitude adjustable between 0 and 2.5 T/m [see Fig. 2(c)]. The static MF was produced by two large permanent magnets of strontium ferrite which are 10 cm distant and produce a static MF ( $\mu_0 H_{DC}$ ) of  $55 \pm 2$  mT [see Fig. 2(d)] (Y30BH, IMA, Spain). This ferrite material was chosen because of its high electrical resistivity ( $>10^4 \Omega \text{ m}$ ), which permits to avoid heating of the magnet by eddy currents generated by the AMF. To superimpose a static MF to the AMF (AMFG), the magnets were placed on both sides of the standard coil (anti-Helmholtz coil).

To check the efficiency of the static MF to prevent MH, 300  $\mu\text{L}$  of the MNP solution presented above were used. This solution was placed inside a 300 kHz uniform AMF. Specific Absorption Rate (SAR) of the MNPs was measured, in the presence or in the absence of a static MF. During the experiment, the temperature increase of the sample submitted to AMF for 60 s was measured using a thermal probe (Reflex, Neoptix, Canada). The temperature of a blank

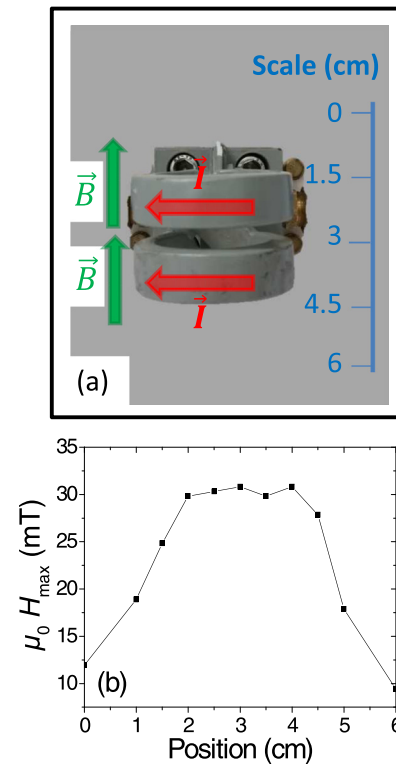


FIG. 1. Magnetic characterisation of the standard coil. (a) Micrograph of the standard coil. (b) Magnetic field amplitude ( $\mu_0 H_{\max}$ ) generated inside the coil with an electric current value of 724 A.

sample containing deionized water was measured in parallel in order to take into account the contribution of the coil warming to the temperature increase. Moreover, to evaluate the contribution of eddy currents to the heating, the temperature of a salted water solution with the same electrical conductivity as the MNP solution ( $\sigma_{\text{MNPs}} \approx 8.1 \text{ mS cm}^{-1}$ ) was also measured. Because there is no magnetic material in this sample, MH is not able to occur and temperature rise is only due to eddy currents. The same experimental protocol was carried out to measure the SAR of MNPs submitted to an AMFG in the presence or not of a static MF. SAR values were calculated using a standard method described in Ref. 31. Dividing SAR values by the magnetic field frequency yielded the specific losses ( $A$ ), expressed in  $\text{mJ/g}_{\text{Fe}}$ . Though salted water solution does not contain any magnetic material, specific losses of this solution were calculated as if it was a MNP solution. This trick allows displaying on the same curve, heating of salted water solution and specific losses of MNP solution in the presence or not of a static MF.

In Fig. 3, the results of SAR measurements in the presence or not of a static MF are shown. Fig. 3(a) displays SAR data obtained under a 300 kHz uniform AMF. As expected, the SAR of the MNPs increases as a function of the AMF amplitude. As observed in this figure, applying a static MF (curve: MNPs with Hdc) decreases the specific losses of MNPs. In this case, two AMF amplitude ranges can be distinguished. First, when  $\mu_0 H_{\max} < \mu_0 H_{DC}$ , the heating of the salted water solution and of the MNPs is equivalent. Under these conditions, heating of the solutions is mainly due to eddy currents and not to the MNPs. This result confirms that, when the AMF amplitude is lower than the static MF

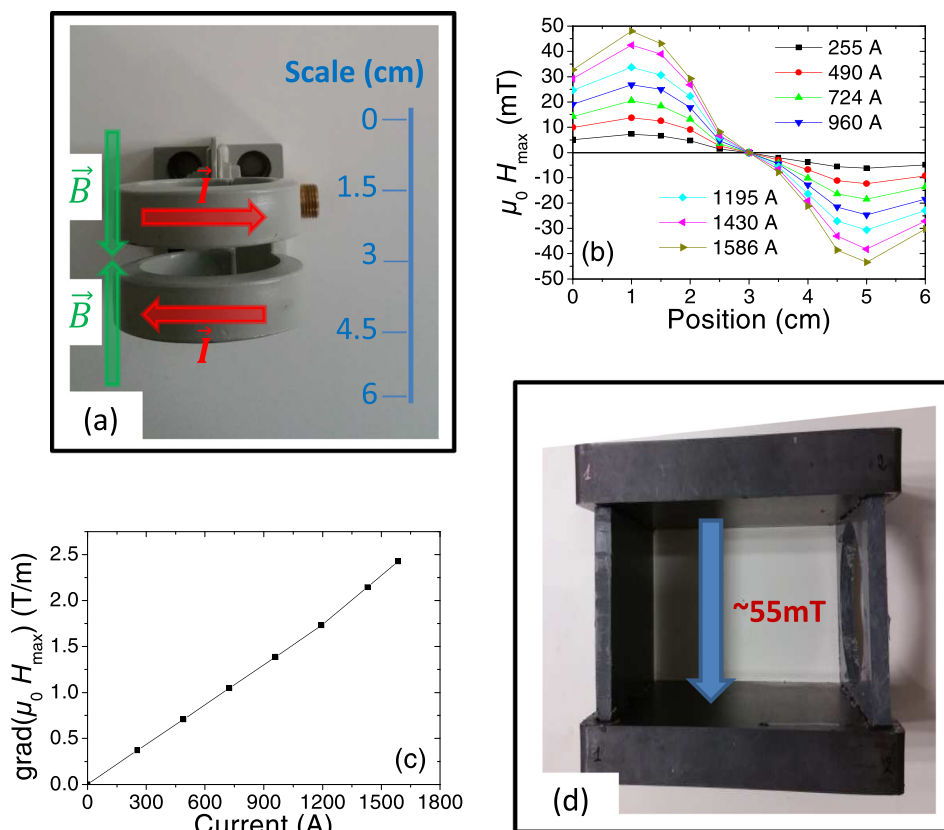


FIG. 2. Magnetic characterisation of anti-Helmholtz coil and static MF. (a) Micrograph of the anti-Helmholtz coil. (b) MF amplitude ( $\mu_0 H_{max}$ ) generated inside the anti-Helmholtz coil for different current amplitudes passing through. “Position” axes refer to the position on the scale shown in (a). Corresponding MF gradients [ $\text{grad}(\mu_0 H_{max})$ ] calculated between positions “1 cm” and “5 cm” are shown in (c). (d) Micrograph of the two ferrite magnets generating a static MF of  $55 \pm 2$  mT.

amplitude, no reversal magnetization of the MNPs and thus no heating by MH occur. Secondly, when  $\mu_0 H_{max} > \mu_0 H_{DC}$ , the MNP solution under a static MF heats more than salted water. This additional heating power is due to MH. It can be noted that the static MF completely prevented MNP heating induced by a 30 mT AMF, which corresponds to the amplitude used in cell death experiments (see below).

Similar measurements were also carried out inside the anti-Helmholtz coil. It should be first remind that, in such a coil,  $\mu_0 H_{max}$  is not constant: for instance, for an AMFG value of 2.5 T/m,  $|\mu_0 H_{max}|$  in coil center (edge) is  $5 \pm 5$  mT ( $45 \pm 5$  mT) [see Fig. 2(b)]. SAR measurements were thus performed at two different positions: at the coil center [see Fig. 3(b)] and at the coil edge [see Fig. 3(c)]. According to Figs. 3(b) and 3(c), the AMF generated by the anti-Helmholtz coil also induced heating of MNPs solution by MH, related to the presence of a non-zero field. As expected, for the same value of AMFG, specific losses of each solution were higher at the coil edge than in the center. As shown in Figs. 3(b) and 3(c), applying a static MF decreases the specific losses. In particular, a static MF of  $55 \pm 2$  mT permits to completely impede the heating of the MNPs, everywhere inside coil and even for the highest AMFG values.

We further analyzed the ability of the different magnetic fields to induce the death of tumor cells. MNPs were grafted with a synthetic analog of gastrin peptide (gastrin-MNPs) in order to specifically target tumor cells expressing the CCK2 receptor (CCK2R), as described in Ref. 13. The tumor cells INR1G9-CCK2R overexpressing the CCK2R were incubated for 24 h with  $16 \mu\text{gFe/ml}$  of gastrin-MNPs enabling their binding and accumulation in cell lysosomes, as described previously.<sup>13</sup> At this concentration, gastrin-MNPs do not present any

cytotoxicity on INR1G9-CCK2R cells.<sup>13</sup> Cells were rinsed and exposed during 1h30 to different magnetic field conditions: either i) an AMF of 30 mT at 300 kHz, as in standard MH experiments, or ii) an AMF of 30 mT at 300 kHz in the presence of the static MF, or iii) an AMFG of 1.4 T/m at 393 kHz in the presence of the static MF, to maximize MNPs translational motion and to prevent MNP heating. Because the anti-Helmholtz coil temperature exceeds  $37^\circ\text{C}$  when the AMFG is beyond 1.4 T/m, biological tests were limited to this value. To minimize eddy currents, the AMF and AMFG were applied in the plane of the Cellview dish. The temperature of the dish was controlled using a thermal probe placed in the incubation medium of the cells. The temperature was maintained at  $37.0 \pm 0.3^\circ\text{C}$  thanks to a home-made temperature regulator and no global temperature rise was measured during AMF or AMFG application. We emphasize that temperature was measured and controlled only at dish-level, which does not provide any information about cell or intra-cell temperature. Control samples were maintained inside a cell incubator. At the end of the experiments, all samples were placed inside a cell incubator for 4 h, and cells were incubated with FITC-annexinV and/or propidium iodure (Cell Meter Annexin V apoptosis assay kit) which identified early apoptotic, late apoptotic, and necrotic cells, respectively. Cells were image analyzed by fluorescence confocal microscopy. The effect of magnetic field treatments on cell death was determined by counting labeled cells from microscopy images representing populations of 2–3000 cells/experiment using ImageJ software. For each condition, the number of labeled cells is expressed as a percentage of total cell population.

As shown in Fig. 4, the application of the AMF at 30 mT and 300 kHz caused the death of cells having internalized

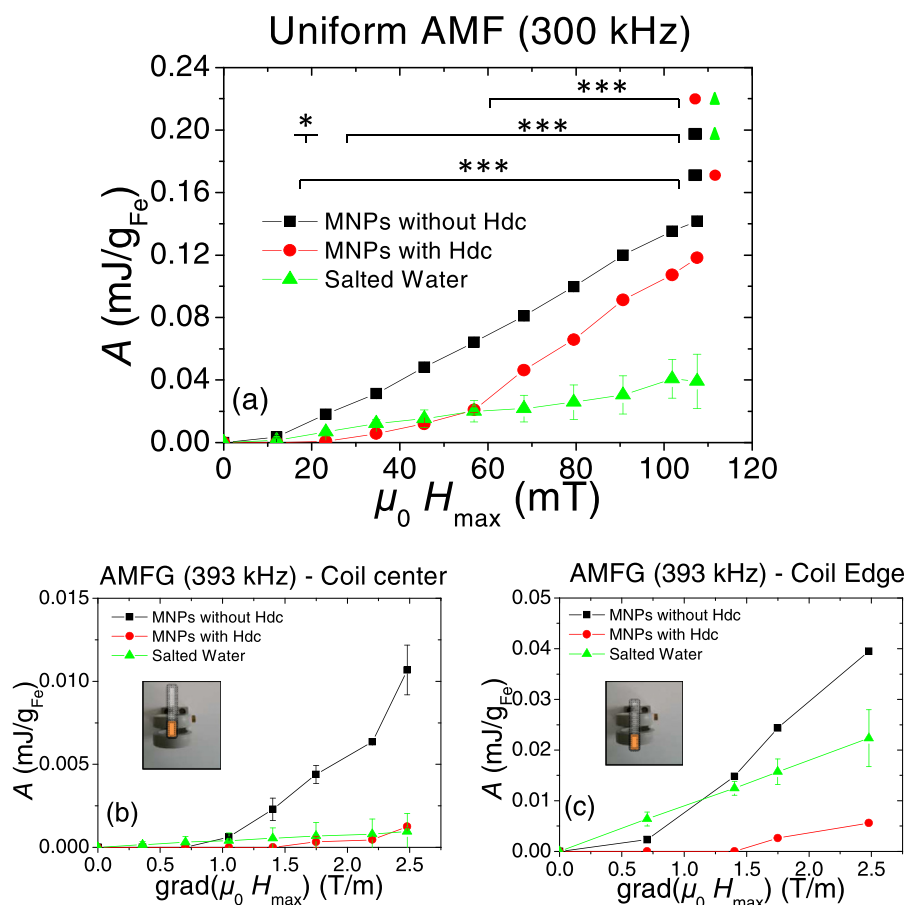


FIG. 3. Specific losses ( $A$ ) measurement of the MNP solution with static MF (MNPs with Hdc - red circle), without static MF (MNPs without Hdc - black square) and salted water solution (Salted Water - green triangle), during AMF ( $\mu_0 H_{max}$ ) or AMFG [ $grad(\mu_0 H_{max})$ ] exposition. Results are the specific losses mean  $\pm$  SEM of two to three separate experiments. (a) Specific loss of MNP and salted water solutions inside an uniform AMF of 300 kHz. Significant differences between each curve are labelled by a number of \*:  $0.01 < p < 0.05$ ; \*\*\*:  $0.0001 < p < 0.001$ . (b) and (c) Specific loss of solutions positioned inside an anti-Helmholtz coil. The AMFG had a frequency of 393 kHz. Insets illustrate the sample position inside the coil. The sample was positioned at the (b) center (c) edge of the coil.

gastrin-MNPs, in agreement with data obtained in Ref. 13. Indeed, exposure to AMF ("AMF without Hdc," in Fig. 4) increased cell death rate of cells having internalized gastrin-MNPs by 2.2 relative to control cells devoid of gastrin-MNPs (% annexinV-PI labeling:  $14.2\% \pm 2.5\%$  vs  $6.5\% \pm 0.8\%$ , respectively). Exposure to the AMF superimposed with a static MF ("AMF with Hdc," in Fig. 4), which prevents MNP heating, does not increase the death rate relative to control (% annexinV-PI labeling:  $7.2 \pm 1.6$  vs  $7.2\% \pm 1.7\%$ , respectively). Thus, we investigated whether translational motion of MNPs could impact on cell viability. Cells were exposed to an AMFG superimposed with a static MF ("AMFG with Hdc," in Fig. 4) which maximizes MNP translational motion and prevents MNP heating. As shown in Fig. 4, the rate of cell death was not significantly increased after exposure to the AMFG superimposed with a static MF relative to control (% annexinV-PI labeling:  $5.6\% \pm 1.5\%$  vs  $5.1\% \pm 1.0\%$ , respectively). All together, these results demonstrate that the cell death rate was not significantly increased comparatively to control cells when a static MF is added: i) to the AMF and ii) to the AMFG. Under these conditions, given the values of AMF and AMFG used, the heating was expected to be negligible (see Fig. 3), but any eventual translational motion maximized, especially for case ii). Thereby, our results strongly support that translational motion of MNPs in lysosomes, even if it is maximized by AMFG, has a negligible impact on cell death induced by an AMF in conditions of MH.

In the introduction, two hypotheses, thermal effect or mechanical effect, were proposed to explain cell death caused by MH. Thermal action hypothesis concerns local

heating of MNPs which occurs at the nanoparticle or lysosome scale and which would trigger a cascade of events leading eventually to cell death through a lysosomal cell death pathway.<sup>14-20</sup> Mechanical action hypotheses concern MNP motions –rotation and/or translational– when an AMF or an AMFG is applied in MH experiments. Data from the current study strongly support that the impact of *translational* motion of MNPs on cell viability is negligible. However, it is important to note that the hypothesis that *rotation* of MNPs could induce cell death is not tested by our experimental protocol and thus cannot be ruled out for the moment. Indeed, during standard MH experiments, MNPs can rotate physically due to torque generated by the AMF.<sup>32</sup> This eventual rotation is blocked when a static MF is applied in addition to AMF. Hence, in experiments combining AMF and static MF, an eventual cell death induced by a torque would also be suppressed. Since MNP physical rotation also drives magnetization reversal and is one of the microscopic mechanisms at the origin of MNP heating, separating the thermal and mechanical contribution to cell death in the case of a rotation seems to be more delicate. What could be used is the fact that the local temperature increase is expected to be mostly linear with the applied frequency, whereas the torque amplitude is, in first approximation, frequency independent. Careful frequency-dependant cell death experiments could thus be used to shed light on this issue.

In summary, our objective was to test the potential impact of the high-frequency MNP translational motion on cell death observed in MH experiments using an AMFG. We took advantage of a static magnetic field which prevents

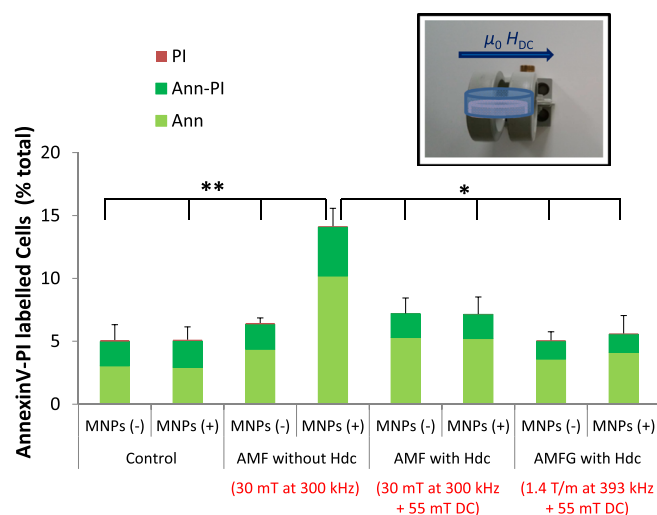


FIG. 4. Biological results. The bar graph shows percentage only annexin (Ann), annexin-propidium iodure (Ann-PI) and only propidium iodure (PI) labelled cells 4 h after MF exposition and for all tested conditions. Respectively, MNPs (+) and MNPs (-) concern cells containing and devoid of gastrin-MNPs. Results are the mean  $\pm$  SEM of three to four separate experiments. \* $0.01 < p < 0.05$ ; \*\* $0.001 < p < 0.01$ . Inset: schematic representation of a CellView dish position inside the coils minimizing eddy current generation. The direction of the static magnetic field (Hdc) is also indicated.

heating of MNPs and maximized MNPs motion when superimposed to AMFG. The absence of MNP heating power when a static MF is applied, in addition to AMF, was confirmed experimentally. Biological experiments demonstrated that the static MF also impedes cell death appearing in MH experiments. Even when translational motion of MNPs was maximized by the use of a dedicated anti-Helmholtz coil, no decrease in cell viability was measured. Thus, the hypothesis ascribing a part of cell death in MH experiment to MNPs translational motion induced by an AMFG is ruled out.

This research was partly funded by CEA Tech Languedoc-Roussillon-Midi-Pyrénées. We thank Cellular Imaging platform of I2MC/INSERM. This research was partly funded by Ligue régionale Contre le Cancer (comité Midi-Pyrénées) and the Cancéropole Grand Sud-Ouest.

<sup>1</sup>R. T. Gordon, J. R. Hines, and D. Gordon, *Med. Hyp.* **5**, 83 (1979).

<sup>2</sup>E. Alphantery, S. Faure, O. Seksek, F. Guyot, and I. Chebbi, *ACS Nano* **5**, 6279 (2011).

<sup>3</sup>S. Dutz and R. Hergt, *Int. J. Hyperthermia* **29**, 790 (2013).

<sup>4</sup>Y. Rabin, *Int. J. Hyperthermia* **18**, 194 (2002).

<sup>5</sup>P. Keblinski, D. G. Cahill, A. Bodapati, C. R. Sullivan, and T. A. Taton, *J. Appl. Phys.* **100**, 054305 (2006).

<sup>6</sup>N. Iovino, A. C. Bohorquez, and C. Rinaldi, *Nanomedicine* **9**, 937 (2014).

<sup>7</sup>M. Creixell, A. C. Bohorquez, M. Torres-Lugo, and C. Rinaldi, *ACS Nano* **5**, 7124 (2011).

<sup>8</sup>M. Domenech, I. Marrero-Berrios, M. Torres-Lugo, and C. Rinaldi, *ACS Nano* **7**, 5091 (2013).

<sup>9</sup>L. Asín, M. R. Ibarra, A. Tres, and G. F. Goya, *Pharm. Res.* **29**, 1319 (2012).

<sup>10</sup>V. Grauzá, A. M. Silber, M. Moros, L. Asín, T. E. Torres, C. Marquina, M. R. Ibarra, and G. F. Goya, *Int. J. Nanomed.* **7**, 5351 (2012).

<sup>11</sup>I. Marcos-Campos, L. Asín, T. E. Torres, C. Marquina, A. Tres, M. R. Ibarra, and G. F. Goya, *Nanotechnology* **22**, 205101 (2011).

<sup>12</sup>L. Asín, G. F. Goya, A. Tres, and M. R. Ibarra, *Cell Death Dis.* **4**, e596 (2013).

<sup>13</sup>C. Sanchez, D. El Hajj Diab, V. Connord, P. Clerc, E. Meunier, B. Pipy, B. Payré, R. Tan, M. Gougeon, J. Carrey, V. Gigoux, and D. Fourmy, *ACS Nano* **8**, 1350 (2014).

<sup>14</sup>J. Dong and J. I. Zink, *ACS Nano* **8**, 5199 (2014).

<sup>15</sup>J. T. Dias, M. Moros, P. del Pino, S. Rivera, V. Grauzá, and J. M. de la Fuente, *Angew. Chem.* **52**, 11526 (2013).

<sup>16</sup>L. Polo-Corralles and C. Rinaldi, *J. Appl. Phys.* **111**, 07B334 (2012).

<sup>17</sup>A. Riedinger, P. Guardia, A. Curcio, M. A. Garcia, R. Cingolani, L. Manna, and T. Pellegrino, *Nano. Lett.* **13**, 2399 (2013).

<sup>18</sup>V. Connord, P. Clerc, N. Hallali, D. El Hajj Diab, D. Fourmy, V. Gigoux, and J. Carrey, *Small* **11**, 2437 (2015).

<sup>19</sup>R. J. Wydra, C. E. Oliver, K. W. Anderson, T. D. Dziubla, and J. Z. Hilt, *RSC Adv.* **5**, 18888 (2015).

<sup>20</sup>C. Zhang, W. Bu, D. Ni, Q. Li, Z. Yao, J. Zhang, H. Yao, Z. Wang, and J. Shi, *Angew. Chem. Int. Ed.* **55**, 2101 (2016).

<sup>21</sup>J. Carrey, V. Connord, and M. Respaud, *Appl. Phys. Lett.* **102**, 232404 (2013).

<sup>22</sup>Y. I. Golovin, S. L. Gribanovsky, D. Y. Golovin, N. L. Klyachko, A. G. Majouga, L. Master, M. Sokolsky, and A. V. Kabanov, *J. Con. Rel.* **219**, 43 (2015).

<sup>23</sup>G. Podaru, S. Ogen, A. Baxter, T. Shrestha, S. Ren, P. Thapa, R. K. Dani, H. Wang, M. T. Basel, P. Prakash, S. H. Bossmann, and V. Chikan, *J. Phys. Chem. B* **118**, 11715 (2014).

<sup>24</sup>G. Podaru, P. Prakash, and V. Chikan, *J. Phys. Chem. C* **120**, 2386 (2016).

<sup>25</sup>B. Mehdaoui, J. Carrey, M. Stadler, A. Cornejo, C. Nayral, F. Delpéch, B. Chaudret, and M. Respaud, *Appl. Phys. Lett.* **100**, 052403 (2012).

<sup>26</sup>P.-M. Déjardin and Y. P. Kalmykov, *J. Magn. Magn. Mater.* **322**, 3112 (2010).

<sup>27</sup>P. M. Déjardin, Y. P. Kalmykov, B. E. Kashevsky, H. El Mrabti, I. S. Poperechny, Y. L. Raikher, and S. V. Titov, *J. Appl. Phys.* **107**, 073914 (2010).

<sup>28</sup>T. O. Tasci, I. Vargel, A. Arat, E. Guzel, P. Korkusuz, and E. Atalar, *Med. Phys.* **36**, 1906 (2009).

<sup>29</sup>M. Ma, Y. Zhang, X. Shen, J. Xie, Y. Li, and N. Gu, *Nano Res.* **8**, 600 (2015).

<sup>30</sup>K. Murase, H. Takata, Y. Takeuchi, and S. Saito, *Phys. Med.-Eur. J. Med. Phys.* **29**, 624 (2013).

<sup>31</sup>L.-M. Lacroix, J. Carrey, and M. Respaud, *Rev. Sci. Instrum.* **79**, 093909 (2008).

<sup>32</sup>H. Mamiya and B. Jeyadevan, *Sci. Rep.* **1**, 157 (2011).